JOURNAL OF OPTOELECTRONICS AND ADVANCED MATERIALS Vol. 9, No. 8, August 2007, p. 2437 - 2444

Optical diode based on unidirectional transmission of defect modes in cholesteric liquid crystals: A simulation study

JIUN-YEU CHEN
Department of Electronic Commerce, Hsing Kuo University of Management, 89, Yuying Street, Tainan 709, Taiwan

A photonic system composed of two cholesteric layers with the same pitch gradient is studied by the finite element method. It is observed that the transmission spectrum can be tailored by incorporating the defects of pitch jump and phase jump in the cholesteric helix. The device is polarization sensitive and exhibits passive anisotropic transmission analogous to the electronic diode. For incident circularly polarized light with the same handedness as the cholesterics, the introduction of the defects in the helical structure leads to the exhibition of unidirectional multiple-band-pass characteristics inside the photonic band gap region. Due to the asymmetrical local resonator cavity, a notable enhancement in the transmission contrast can be realized. Some critical parameters for the non-reciprocal transmission behavior are demonstrated theoretically: the apodization function, the thickness of the double composite film, and the twist angle. In addition, the defect wavelengths in the transmission spectrum can be tuned linearly by adjusting the amount of the phase jump. Equipped with a different phase jump according to the linear behavior, it is easy for the optical diode to control the unidirectional transmission channels.

(Received March 5, 2007; accepted June 27, 2007)

Keywords: Optical diode, Photonic crystal, Cholesteric liquid crystal, Defect mode, Apodization

1. Introduction

Dielectric materials with a periodic modulation of the refractive index can exhibit a photonic band gap (PBG), in which a certain frequency range of light is forbidden along the propagation direction. Such artificial optical media are known as photonic crystals (PCs). When a defect is introduced in a PC, localization of photons can be achieved [1]. PBGs and defects, which can be used to confine and manipulate photons, may realize the creation of all-optical integrated circuits. Because of their analogies with semiconductors and their potential to advance photonic technology, PCs have various interesting technological applications in many areas of physics and engineering, including photonic chips, microsources, holey fibers, and nonlinear optics [2,3].

Among many PBG materials, chiral photonic crystals with helical structures are very attractive. Cholesteric liquid crystals (CLCs) and ferroelectric liquid crystals can be synthesized by an appropriate chemical mixture to self-organize [4,5]. Sculptured thin films (STFs) can be constructed by physical vapor deposition [6]. Besides, the incorporation of chirality into the quarter-wave reflector can produce different band structure for each polarized light [7]. The selective reflection band for circularly polarized light in the direction of structural anisotropy is created by coherent multiple scattering on distributed Bragg reflection structures. A circularly polarized light with the same handedness as the cholesterics propagating along a helical axis is forbidden in the pseudo-bandgap, and light of opposite chirality is unaffected by the structure [8]. In the planar texture of CLCs, the axes of molecular director rotate from plane to plane to form a helical structure with pitch P. For sufficiently thick films, the reflectance of a specific polarized light with normal incidence is nearly 100% within a band centred at $\lambda_o = \overline{n}P$. The bandwidth is $\Delta\lambda \approx \lambda_o \Delta n / \overline{n}$, where $\Delta n = n_{\|} - n_{\perp}$ is the birefringence defined by the indices of refraction parallel and perpendicular to the nematic director and $\overline{n} = [(n_{\|}^2 + n_{\perp}^2)/2]^{1/2}$ is the average. A rich variety of defects introduced into the perfect helical structure have been proposed [9]. A defect can be created by inserting an optically isotropic or anisotropic layer in CLCs. By the discontinuity in the helix, a twist defect results in the localized modes at the position of the defect. Based on numerical analyses, the modulation of helical twisting power via the local deformation of the helix in the CLC layer can also create photonic defect modes [10]. In a hybrid system consisting of CLC layers with different pitches, the defect modes appear at the band edge of the sandwiched CLC layer [11]. Defect modes in chiral PCs have received much attention and may be used for narrow band filters and low threshold lasers [12,13].

In electronic circuits, an electronic diode is an

essential element that permits a current in one direction but not the other. A device can be defined as an optical diode (OD) if it prevents the backward propagation of a light beam and allows the forward propagation. Generally, an OD is preferably arranged between the laser and the optical fibre to suppress the backward reflection of the light beam caused by the ends of the optical fibres. One of the familiar optical instruments using this effect is the Faraday rotator. Various ODs based on photonic crystal structures have been proposed and demonstrated. One theoretical model is a nonlinear thin-film multilayer device which possesses a gradient refractive index modulation [14]. ODs can also be composed of multilayer systems with gyrotropic layers [15]. If an extremely anisotropic system possesses dielectric and magnetic helicities, the coexistence of optical and magnetooptic activities can lead to irreversibility effects. The system subjected to a magnetic field can function as a perfect OD [16]. Coupled photonic defects with nonlinearity have been theoretically studied to show the unidirectional transmission behaviour [17]. An asymmetric multilayer structure formed by alternating two dielectric materials with positive and negative refractive indices exhibits spatially non-reciprocal transmission of electromagnetic waves [18]. Characteristic PBG structures corresponding to the combination of CLC layers and wave-plates show the diode action for a specific polarization state of light [19]. The tunability in OD operation has been designed to show electro-controlled unidirectional transmission [20,21]. In sum, the diode behaviour depends on complex asymmetric structures, nonlinear properties, metamaterials, and polarization states.

Since there is no simple in-line polarization filter which can filter orthogonal polarizations without the requirement of external fields, the assembling devices are insensitive to the polarization state of the light field in most optical circuits. Chiral PCs with defects can provide a way for accomplishing bandpass circular-polarization filters with the polarization-dependence of the narrow transmission features. The polarization-dependent structure investigated in this article is capable of realizing multiple-wavelength filtration and can be equipped for acting as an OD. Making the structure asymmetric is the general idea to achieve directional propagation of light. In our previous study, the inclusion of defects introduced by a pitch jump and a helical phase jump in a stacked structure of two CLC layers with spatially varying period has been analysed for the purpose of multiple-wavelength filtration [22]. Here, the significant transmission contrast on the photonic defect modes is emphasized to demonstrate the possibility of unidirectional action. Apodized chiral structures can be built up out of simple elements via using the finite element method (FEM) for numerical simulations. It is believed that this chiral photonic diode can provide some striking advantages over the other proposals because of its simplicity and no energy requirements.

2. Model structure

A photonic structure can be made to vary spatially by changing the lattice repeat distance. The spatially varying structure can provide reflection over a broader range of the photonic stop band than a simple periodic structure [23]. Figure 1(a) shows the apodized structure in a CLC layer. A single CLC layer can be assumed to have an exponentially varying pitch $P(z)$, and the apodization function for the directions *I* and *II* can be expressed as [24]

$$P_{I,II}(z) = P_{\mp} \exp(\frac{\pm z}{d} \ln \gamma), \quad (1)$$

where d is the thickness, and γ is the ratio of the largest and the smallest pitches (P_+ / P_-). Since cholesterics are locally nematic and fluid, chiral nematic liquid crystals (LCs) with a spatially varying pitch must be solidified to stabilize the PBG properties. Polymer films with a stable LC order can be produced by combining thermal gradient and UV-crosslinking reaction in a CLC mixture [23], photopolymerizing LC monomers [25], and quenching CLC oligomers [26].

Linear optical properties of apodized structures can be modeled by using the Galerkin FEM [27]. The Maxwell equations can be used to simulate the light propagation in the medium with refractive index varying along the propagating direction. Based on Berreman's method, the time-independent equation for the electric field $\mathbf{E} = (E_x, E_y)^T$ along the helical z-axis is given by [22]:

$$\frac{d}{dz}\left(\frac{1}{k_0}\underline{\underline{\Delta}}_H \frac{d}{dz}\mathbf{E}\right) + k_0 \underline{\underline{\Delta}}_E \mathbf{E} = 0, \quad (2)$$

where

$$\underline{\underline{\Delta}}_H = \begin{bmatrix} 0 & \left(\frac{k_x^2}{k_0^2}\frac{1}{\varepsilon_\perp} - 1\right) \\ 1 & 0 \end{bmatrix}^{-1}, \quad (3)$$

$$\underline{\underline{\Delta}}_E = \begin{bmatrix} s\delta \sin 2(\beta z + \alpha) & \left(\varepsilon - \delta \cos 2(\beta z + \alpha)\right) - k_x^2 / k_0^2 \\ -\left(\varepsilon + \delta \cos 2(\beta z + \alpha)\right) & -s\delta \sin 2(\beta z + \alpha) \end{bmatrix}. \quad (4)$$

Here $\beta = 2\pi / P(z)$, $\varepsilon \equiv (\varepsilon_{\parallel} + \varepsilon_{\perp})/2$, $\delta \equiv (\varepsilon_{\parallel} - \varepsilon_{\perp})/2$,

and α is used for the phase jump of the twist defect. $\varepsilon_{\parallel}$ and $\varepsilon_{\perp}$ are the dielectric constants parallel and perpendicular to the nematic director, respectively. s=1 is the right-handed screw sense and s=-1 is the left-handed one. For the incident light with wavelength λ at an oblique angle θ relative to the z-axis, the wavenumber is $k_0 = 2\pi/\lambda$ and its component in the x-direction is $k_x = k_0 \sin\theta$. Galerkin's method is applied to Eq. (2) to obtain the matrix equations of the FEM.

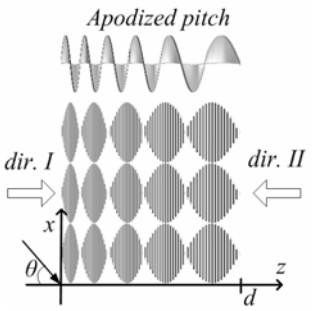

a

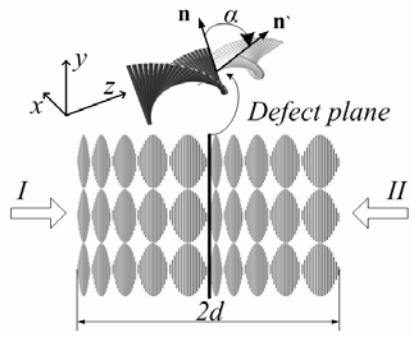

b

Fig. 1. Sketches of helical structures with apodized pitch. (a) A single CLC layer with spatially varying pitch. (b) A pitch jump and a helical phase jump with a twist angle α are introduced into the helix of the stacked CLC layers. n and n` are the nematic directors. The open arrow indicates the light propagating direction.

A simple framework is shown in Fig. 1(b) where the OD device is a stacked structure of two CLC layers with the same spatially varying period. The apodized pitch is assumed to have an exponential profile given in Eq. (1). The PC defects are introduced by a pitch jump and a helical phase jump in the middle of the structure. To evaluate the performance of the device, the following parameters are selected in the calculation. The indices of refraction parallel and perpendicular to the nematic director are chosen to be $n_{\parallel} = 1.7$ and $n_{\perp} = 1.5$. It is assumed that the sample is nearly index matched to its surroundings with $n_s = \sqrt{(n_{\parallel}^2 + n_{\perp}^2)/2}$. The smallest and the largest pitches are taken to be P_{-}=900 nm and P_{+}=1080 nm for the adjustment of the "full-wave" reflection band to cover the range of transmission bands from the S-band (1460−1530 nm) to the U-band (1625−1675 nm). The handedness of the host CLC in the whole study is assumed to be right. For achieving higher accuracy, Lagrange-quadratic elements are chosen as the basis elements. The absorbing boundary condition is adopted in the FEM model.

3. Bragg reflection of an apodized chiral structure

To establish a circular Bragg reflection for normally incident circularly polarized light, a minimum cholesteric layer thickness is required [28]. In Fig. 2, the simulated transmission spectrum of an apodized cholesteric structure sketched in Fig. 1(a) is shown for the light of right circular polarization (RCP) in different propagating directions. The thickness for the simulations is $d = 30P_{-}$. Solid and dotted lines in the spectrum are plotted for the directions *I* and *II*, respectively. The variation of the pitch gradient would lead to varying the reflection wavelength. The variation of the reflection wavelength according to the different gradient direction can be expressed as a linear form [24]:

$$\Delta\lambda_{I,II} = \overline{n}\left(\frac{dP(z)}{dz}\right)_{I,II}\Delta z\,. \qquad (5)$$

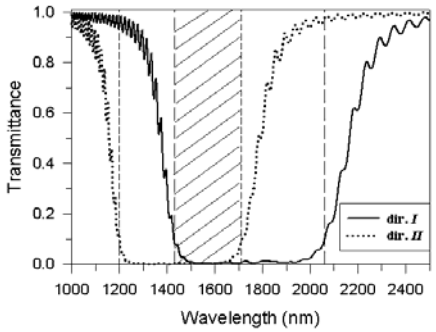

Fig. 2. Transmission spectrum of RCP light for an apodized cholesteric structure sketched in Fig. 1(a). Solid and dotted lines in the spectrum are plotted for the directions I and II indicated in Fig. 1(a), respectively. The PBG in the direction I (II) is bounded by the long-dashed (short-dashed) lines. The shadow of diagonal lines, which is located between 1430 and 1710nm, is supposed as a FWBG in a single CLC layer for the incident light of RCP.

The stop band in Fig. 2 will be located within $\overline{n}P_{-} \sim \overline{n}P_{+} + \Delta\lambda_I$ (from 1430 to 2060nm) for the curve of the direction *I* and within $\overline{n}P_{-} + \Delta\lambda_{II} \sim \overline{n}P_{+}$ (from 1200 to 1710nm) for that of the direction *II*. In the schematic structure of Fig. 1(a), it can be supposed that a "full-wave" band gap (FWBG) for the incident light of RCP would be located between $\overline{n}P_{-}$ and $\overline{n}P_{+}$ as shown in the shadow of Fig. 2. The wavelength range of a FWBG in such a structure can be controlled by adjusting P_{-} and P_{+}. In this study, the FWBG is around 1430-1710nm (transmittance under 0.1).

4. Transmission behaviour of a discontinuous pitch variation

The simulations of the transmission in the stacked CLC layers containing only a pitch jump in the middle of the structure are presented in Fig. 3(a) and Fig. 3(c) for the thicknesses of $2d = 15P_{-}$ and $18P_{-}$, respectively. Figure 3(b) and Fig. 3(d) show the enlarged views of Fig. 3(a) and Fig. 3(c), in which they are confined to the range of the FWBG. In both cases for normal incident light of RCP, defect modes are generated by the pitch jump in the FWBG. The difference between the light propagation directions leads to different centre resonance wavelengths of the defect modes. In the FWBG as shown Fig. 3(b), the transmission spectrum in the direction *I* peaks at the labels **A** and **C** (centred at ~1470 and ~1585nm), with the full widths at half maximum (FWHMs) of 25 and 11nm, whereas that in the direction *II* peaks at the labels **B** and **D** (centred at ~1496 and ~1624nm), with the FWHMs of 6 and 19nm. The separation between two peaks is at least 25 nm and the overlap is quite small. The defect modes become sharper near the centre of the FWBG. The effective transmission takes place along the direction *I* for some defect wavelengths and along the direction *II* for others. Thus the component functions as a diode. The RCP light transmittance of the defect mode for the direction *I* (*II*) output is T^{I}_{RCP} (T^{II}_{RCP}). The unidirectional transmission behaviour can be expressed by the transmission contrast defined as $C_I = T^{I}_{RCP} / T^{II}_{RCP}$ and $C_{II} = T^{II}_{RCP} / T^{I}_{RCP}$ to characterize the efficiency of the OD. In each defect mode shown in Fig. 3(b), the transmission contrast C_I for the labels **A** and **C** is 69 and 38, and C_{II} for the labels **B** and **D** is 6 and 28. It is noticed that the centre wavelengths of the defect modes depend on the thickness of the stacked structure and the maximum peak values of all defect modes almost reach unity. With the increase of the thickness, the number of the defect modes is larger, and the peaks of the defect modes become sharper. There is no distinct defect mode observed for normal incident light of left circular polarization (LCP) in the directions *I* and *II*.

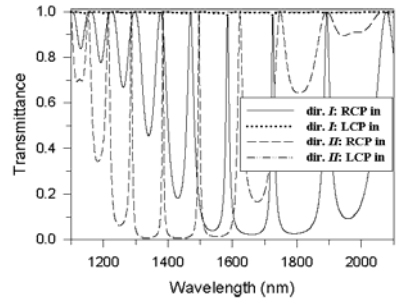

a

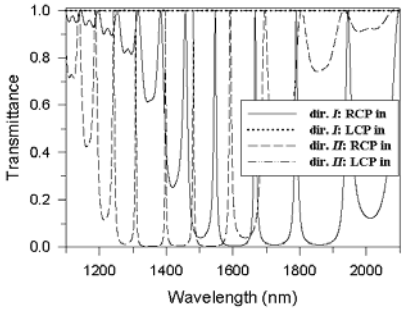

b

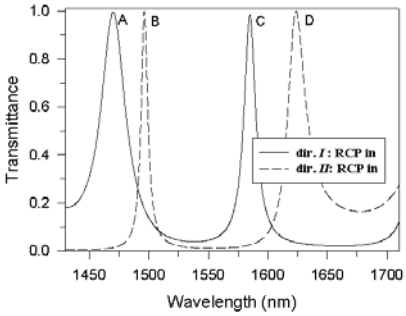

c

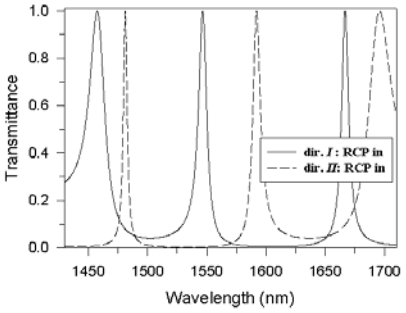

d

Fig. 3. Transmission spectra of the stacked CLC structure with apodized pitch (Fig. 1(b)) for normal incident light of RCP and LCP in the directions I and II. Only a pitch jump is introduced into the cholesteric helix. The total thickness for (a) and (c) is 2d=15P- and 18P-, respectively. (b) and (d) show the enlarged views of (a) and (c), in which they are plotted in the range of the FWBG.

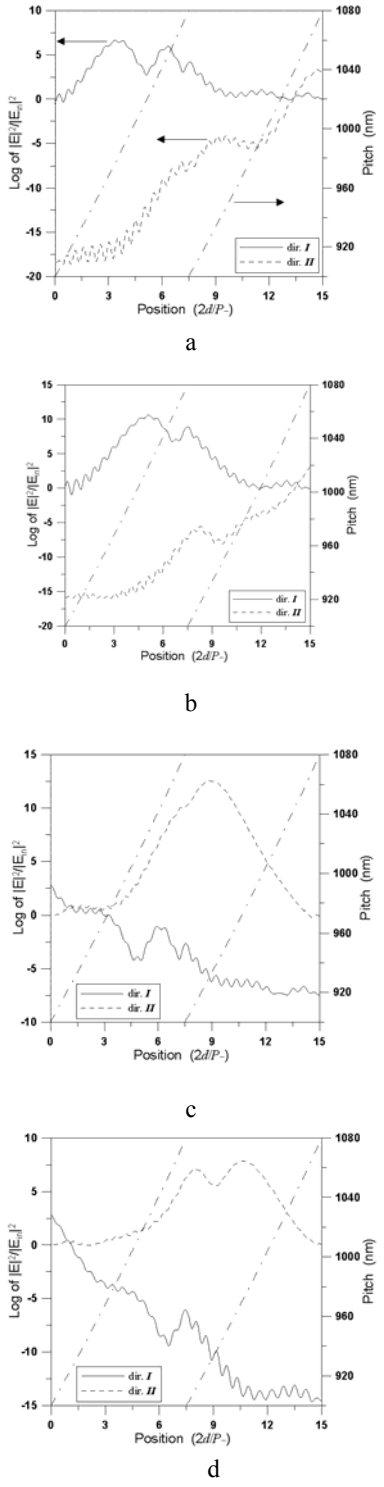

Fig. 4. Distribution of the relative squared modulus of the electric field inside the double-composite film for the defect modes indicated in Fig. 3(b). The energy distribution corresponding to the centre wavelengths of the labels A−D is shown in (a) − (d). The pitch inside the stacked CLC structure is shown by the dotted-dashed lines.

The OD effect at the chiral defect resonance can be better understood by considering the spatial distribution of energy inside the sample. For excitation at the centre resonance wavelengths shown in Fig. 3(b), the spatial dependence of the logarithmic relative squared modulus of the electric field for the defect modes is sketched in Fig. 4. The corresponding pitch inside the stacked CLC structure is also plotted in Fig. 4. The distribution of the energy intensity for the different defect modes along the distinct directions corresponds to a relative position of a resonator cavity formed by the double composite film [22]. The figures show that the resonance condition along one direction is quite different than that along the other. The apodization in the pitch shifts the resonator cavity and results in the non-reciprocal transmission of the defect modes in the FWBG. In Fig. 4(a) for the case of the label **A** (Fig. 3(b)), the incident RCP light along the direction *I* can easily reach its corresponding resonator cavity to excite the localized mode and pass through the structure. However, the effect of the apodization pushes the cavity away from the rear side so that the incident RCP light along the direction *II* hardly reaches the cavity with respect to its eigen mode. The defect mode cannot be effectively excited, and therefore the intensity never rises high enough to penetrate the PGB. In the other cases of defect modes, the essential transmission of the incident RCP light in either direction can also be reasoned by analogy.

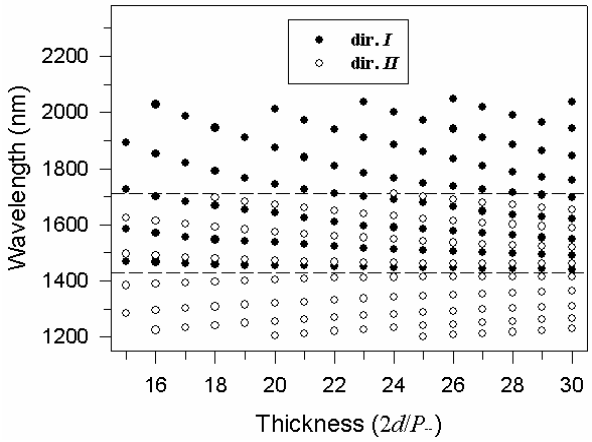

Fig. 5. Thickness dependence of the centre wavelengths of the defect modes for the incident light of RCP in both directions. Only a pitch jump is introduced into the cholesteric helix. The FWBG is bounded by the dashed lines.

As regards the effect of the double composite film thickness, Fig. 5 shows the centre wavelengths of the defect modes as a function of thickness for the incident light of RCP in both directions. It was found that the localized modes could be well confined in the FWBG when the structure thickness is greater than $2d = 15P_{-}$. With the increase of the structure thickness, the number of the defect modes becomes large, and the resonant modes are shifted toward the FWBG. All peak values of the defect modes are close to unity from the thickness $2d = 15P_{-}$ to $30P_{-}$, and no obvious defect mode is observed for normal incident light of LCP. For either direction, the centre wavelength λ_{ν} of each mode existing in the FWBG could be estimated by the following relation [22]:

$$\frac{1}{\lambda_{\nu+1}} - \frac{1}{\lambda_{\nu}} = \frac{1}{2\bar{n}\Delta d}, \tag{6}$$

where $\lambda_{\nu} > \lambda_{\nu+1}$ and $\Delta d \approx d$. In order to obtain a large transmission contrast in the OD, it is needed to use a larger structure thickness to enhance the defect mode in the forward direction but to suppress it in the backward one. Further, the peaks of the defect modes in either direction would be much closer to each other, and the overlap is still small. Multiplex unidirectional transmission channels thus can be achieved. However, the increase of thickness is restricted by the effect of the anomalous crossover behaviour [22].

5. Transmission behaviour of a combination of discontinuous pitch variation and twist defect

In the model with the defect of a combination of a pitch jump and a phase jump (Fig. 1(b)), figure 6 shows the transmission spectra of incident RCP light in both directions for the different twist angles α=0°, 45°, 90°, and 135°. The thickness of the stacked layers is $2d = 18P_{-}$. It can be observed that the shifts of the defect modes results from the phase jump. In general, increasing the phase jump from 0° to 180° gives rise to the shift of the resonance wavelength from the long wavelength band edge to the short wavelength band edge in the constant pitch cholesterics with a twist defect [9]. The similar phenomenon of the shift in wavelength for the defect modes in the stacked CLC layers with apodized pitch also reveals in Fig. 6(a). Nevertheless, in Fig. 6(b) for the oppositely propagating direction, the twist defect in the cholesteric helix shifts the defect modes to longer wavelengths. The maximum transmittance of the defect modes nearly keeps constant for all twist angles. The unidirectional narrow pass-bands could be tuned by this characteristic. Further, attaching the CLC layers to individual substrates and joining the two slabs with index-matching oil could be extended to the application of tunable unidirectional filters via a tuning mechanism. However, the concept cannot be implemented by the STF technology due to the special nano-engineering process [6].

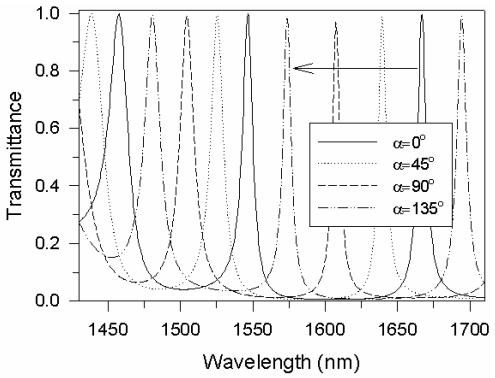

a

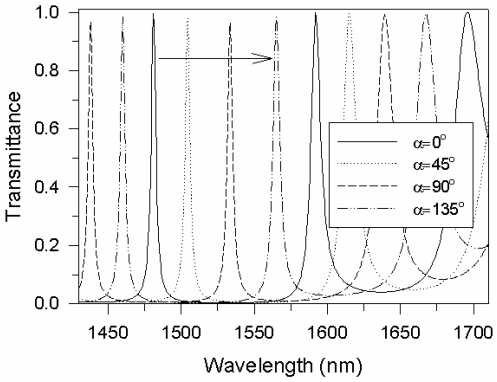

b

Fig. 6. Transmission spectra of the stacked CLC structure containing combined defects of a pitch jump and a helical phase jump, assuming the total thickness $2d = 18P_{-}$ and phase jumps α=0°, 45°, 90°, and 135°. The variation of the spectra for the incident light of RCP in the directions I and II is shown in (a) and (b), respectively.

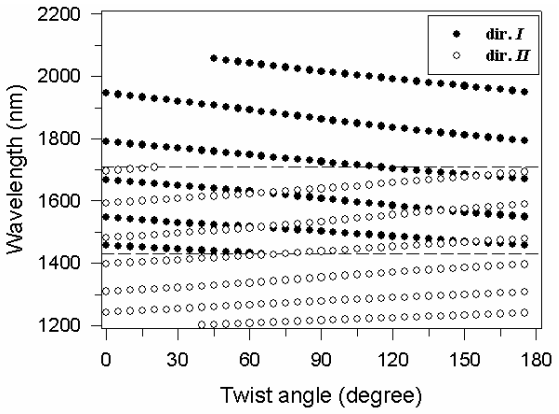

Fig. 7. Dependence of the centre wavelengths of the defect modes on the twist angle for normal incident light of RCP in both directions. The thickness of the stacked CLC structure is taken as $2d = 18P_{\_}$. *The FWBG is bounded by the dashed lines.*

To show the continuous modulation of the twist angle α, Fig. 7 shows the twist angle dependence of the centre wavelengths corresponding to the defect modes for the incident RCP light in both directions. The thickness of the stacked layers is $2d = 18P_{\_}$ in the simulations. In this case, the sweep in wavelength is focused on the FWBG, and the defect wavelengths from the long/short to the short/long wavelength can be tuned by varying the twist angle from 0˚ to 180˚. The maximum transmittance of the defect modes for all angles is almost equal to unity for incident RCP light. It is important to note the linearity of the sweep in angle as shown in Fig. 7. This effect can be considered so as to control the pass-band shift of the unidirectional filter. However, it should be noted that there is no OD effect for some defect modes at a certain twist angle (60˚–70˚ and 140˚–155˚). Even if the apodization leads to asymmetric transmission, the resonator cavity for a specific wavelength could be shifted to the same position by the phase jump in different directions. The same defect mode would be excited in either direction, and then the OD performance disappears.

6. Conclusions

It has been studied in this work that the effect of the defects introduced by a pitch jump and a phase jump in a stacked CLC structure with apodized pitch could lead to unidirectional light propagation. The structure is polarization sensitive at normal incidence since it is made up of chiral media. In the FEM simulations, the apodization in the cholesteric helix can shift the defect modes in the double composite layer for forward and backward light propagation. The transmission of specific circularly polarized radiation at the defect wavelengths strongly differs for incidence from the two sides, which is a major feature of an OD. Beside, the inclusion of the defect introduced by a pitch jump in the helical structure gives rise to multiplex narrow-band transmission within the FWBG. The defect modes change with the increase in thickness and in the phase jump applied to the helical structure. The sharpness and the pass-bands of the localized modes in the transmission spectrum can be chosen by varying the thickness of the stacked CLC layers, which is one of the most critical parameters. The other important parameter is the twist angle in the discontinuity of the cholesteric helix. The phase jump determines a greater sweep in wavelength as it is increased with a region of linearity from 0˚ to 180˚. The linearity response in the defect modes to the twist angle is appreciated for a tunable OD. These dependences can be nano-manufactured and tested in real experiments. Such a device shows promising photonic applications in a variety of areas as optical polarization filtration, optical isolation, and all-optical processing.

Acknowledgements

The author acknowledges the National Science Council (NSC) of Taiwan for financial support under contract No. NSC 95-2221-E-432-001.

References

[1] J. D. Joannopoulos, R. D. Meade, J. N. Winn, Photonic Crystals: Modeling the Flow of Light, Princeton University Press, Princeton, NJ (1995).
[2] H. Rigneault, J.-M. Lourtioz, C. Delalande, A. Levenson, Nanophotonics, ISTE, London (2006).
[3] M. Soljačuć, J. D. Joannopoulos, Nature Mater. **3**, 211 (2004).
[4] P. V. Shibaev, V. I. Kopp, A. Z. Genack, J. Phys. Chem. B **107**, 6961 (2003).
[5] M. Ozaki, M. Kasano, D. Ganzke, W. Haase, K. Yoshino, Adv. Mater. **14**, 306 (2002).
[6] K. Robbie, J. C. Sit, M. J. Brett, J. Vac. Sci. Technol. B **16**, 1115 (1998).

[7] P. Tran, J. Opt. Soc. Am. B **16**, 70 (1999).
[8] P. G. de Gennes, J. Prost, The Physics of Liquid Crystals, 2nd edn., Clarendon Press, Oxford (1993).
[9] J. Schmidtke, W. Stille, Eur. Phys. J. E **12**, 553 (2003).
[10] H. Yoshida, R. Ozaki, K. Yoshino, M. Ozaki, Thin Solid Films **509**, 197 (2006).
[11] R. Ozaki, T. Sanda, H. Yoshida, Y. Matsuhisa, M. Ozaki, K. Yoshino, Jpn. J. Appl. Phys. **45**, 493 (2006).
[12] V. I. Kopp, Z.-Q. Zhang, A. Z. Genack, Progress in Quan. Electron. **27**, 369 (2003).
[13] V. Barna, S. Ferjani, A. De Luca, R. Caputo, N. Scaramuzza, C. Versace, G. Strangi, Appl. Phys. Lett. **87**, 221108 (2005).
[14] M. D. Tocci, M. J. Bloemer, M. Scalora, J. P. Dowling, C. M. Bowden, Appl. Phys. Lett. **66**, 2324 (1995).
[15] G. A. Vardanyan, A. A. Gevorgyan, Opt. Spectrosc. **99**, 992 (2005).
[16] A. H. Gevorgyan, Tech. Phys. **47**, 1008 (2002).
[17] X.-S. Lin, W.-Q. Wu, H. Zhou, K.-F. Zhou, S. Lan, Opt. Express **14**, 2429 (2006).
[18] M. W. Feise, I. V. Shadrivov, Y. S. Kivshar, Phys. Rev. E **71**, 037602 (2005).
[19] J. Y. Chen, L. W. Chen, Opt. Express **14**, 10733 (2006).
[20] J. Hwang, M.H. Song, B. Park, S. Nishimura, T. Toyooka, J.W. Wu, Y. Takanishi, K. Ishikawa, H. Takezoe, Nature Mater. **4**, 383 (2005).
[21] M. H. Song, B. Park, Y. Takanishi, K. Ishikawa, S. Nishimura, T. Toyooka, H. Takezoe, Thin Solid Films **509**, 49 (2006).
[22] J. Y. Chen, L. W. Chen, Phys. Rev. E **71**, 061708 (2005).
[23] A. Lavernhe, M. Mitov, C. Binet, C. Bourgerette, Liq. Cryst. **28**, 803 (2001).
[24] J. Y. Chen, L. W. Chen, Physica B **357**, 282 (2005).
[25] M. Mitov, E. Nouvet, N. Dessaid, Eur. Phys. J. E **15**, 413 (2004).
[26] D. J. Broer, G. N. Mol, J. A. M. M. van Haaren, J. Lub, Adv. Mater. **11**, 573 (1999).
[27] J. Jin, The Finite Element Method in Electromagnetics, Wiley, New York (2002).
[28] D. -K. Yang, S. -T. Wu, Fundamentals of Liquid Crystal Devices, Wiley, Chichester (2006).

*Corresponding author: n1888112@nckualumni.org.tw